Fast 2.5D Loss Calculation for round Litz Wires

Luo, Tianming; Ghaffarian Niasar, Mohamad; Vaessen, Peter

Citation (APA)
Luo, T., Ghaffarian Niasar, M., & Vaessen, P. (2023). Fast 2.5D Loss Calculation for round Litz Wires. *IEEE Transactions on Magnetics*, *60*(3), 1-4. Article 6300804. https://doi.org/10.1109/TMAG.2023.3329169

Important note
To cite this publication, please use the final published version (if applicable).
Please check the document version above.

Fast 2.5-D Loss Calculation for Round Litz Wires

Tianming Luo[1], Mohamad Ghaffarian Niasar[1], and Peter Vaessen[1,2]

[1]Department of Electrical Sustainable Energy, Delft University of Technology, 2628 CD Delft, The Netherlands
[2]KEMA Laboratories, 6812 DE Arnhem, The Netherlands

Litz wire, which is used to suppress eddy current, always have complex structure. Solving its 3-D finite element model (FEM) requires high computational resources. This article presents a 2.5-D loss calculation method for round Litz wires, which do not need mesh. One pitch of Litz wire is set as an object. The exact structure is constructed by a recursive method and then is sliced into several sections per pitch. Each section is represented by a cross section area. Two-dimensional problems are solved based on an analytical method, which is based on magnetic vector potentials in quasi magneto-statics situation. One pitch of the Litz wire is approximately represented by the summation of 2-D problems. The proposed method is compared with 3-D FEM results, which shows the proposed method has good accuracy and fast computational speed.

Index Terms— **Copper losses, eddy current, proximity effect, skin effect.**

I. Introduction

WINDING losses are essential parts of the losses in magnetic components. In medium-frequency applications, eddy current cannot be neglected as low frequency. To achieve high efficiencies, Litz wires are widely used to suppress the eddy current. It comprises dozens or hundreds strands, which are twisted together through complex construction. Through twisting, Litz wires can dramatically reduce the proximity effect losses caused by the external magnetic field and average the current allocation in strands.

In order to select suitable Litz wires, accurate loss estimation is necessary. Most models [1], [2], [3], [4] assume the twist is perfect and each strand has the same proximity losses and current. However, Sullivan and Zhang [5] indicated the twist cannot achieve perfect performance, and proposed an analytical method to consider the twist effect. Three-dimensional finite element model (FEM) generally can provide accurate results [6], but it requires high computation resources and long computational time. In order to accelerate the computational speed, methods like partial element equivalent circuit (PEEC) [7], [8], [9], homogenization [3], 2.5-D approximation [10] and thin wire approximation [11] are employed. In methods [9], formulas from [1] are used to reduce discretization effort, which at the same time ignores the interaction between eddy currents.

This article presents a 2.5-D loss calculation method for round Litz wires, which shares the same idea with [10]. The advantage is that the proposed method is based on an analytical solution and does not need discretization procedures. Therefore, the proposed method can provide faster calculation time and similar accuracy compared to [10], which uses 2-D FEM. The 2.5-D method assumes the twisting far from the targeted section does not cause much deviation from the 2-D situation, and the longitudinal current plays a dominant role.
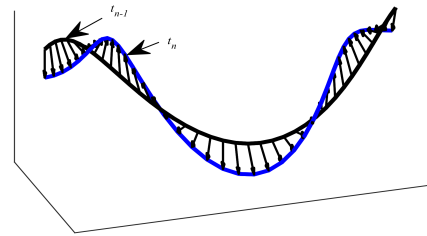
Fig. 1. Illustration of the relation between two level's tracks.

Litz wire's strands mainly extend in the longitudinal direction, which complies with this assumption.

The article is structured as follows. Section II introduces the building of the 3-D construction of Litz wire, 2-D analytical model, and loss calculation procedure. Section III gives two case studies, and compares the results from the proposed method, 3-D FEM, and two other methods.

II. Calculation Procedure

A. Litz Wire Construction and Slicing

The first step is constructing the structure. A recursive multilevel bundle structure [12] is adopted. The method is briefly introduced in this section. In general, each level's trajectories are decided by the previous level's trajectory and the radius of this level bundle's position, as shown by Fig. 1. This relation can be described by the following equation:

$$t_n(x, y, z) = t_{n-1}(x, y, z) + R_{n,\text{pos}} \cos(\lambda_n \varphi) \cdot \overrightarrow{n_{n-1}}$$
$$+ R_{n,\text{pos}} \sin(\lambda_n \varphi) \cdot \overrightarrow{b_{n-1}} \quad (1)$$

where $t_n(x, y, z)$ is the trajectory of nth level bundle, φ is the global curve parameter in the range of 0–2π, $R_{n,\text{pos}}$ is the bundle's position, λ_n is the ratio of the nth level bundle's pitch to the global wire pitch, and $\overrightarrow{n_{n-1}}$ and $\overrightarrow{b_{n-1}}$ are two normalized vectors in Frenet–Serret frame, which is perpendicular to the $n - 1$th level bundle's curve. Several conditions from [6] and [7] are used to avoid the overlapping of trajectories.

After constructing one pitch of Litz wire, the construction is sliced into several sections, and each section is represented by a cross section of Litz wire, as shown
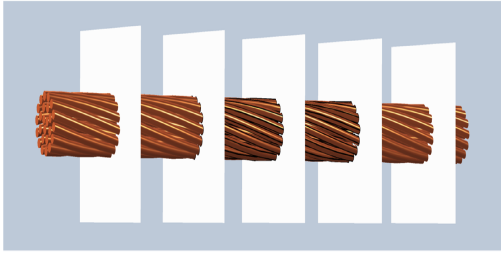
Fig. 2.   Illustration of slicing the Litz wire into sections.

in Fig. 2. Then, the 3-D Litz wire model becomes several 2-D models. In the shown cases, one pitch is sliced into ten sections, which is generally enough according to our experience.

B. Two-Dimensional Multi-Conductor Model

To solve 2-D questions, the following partial differential equation (PDE) is used based on magnetic vector potential A in quasi magneto-statics. ω, σ and μ are angular frequency, conductivity and permeability, respectively

$$\nabla^2 A - j\omega\sigma\mu A = \mu\sigma\nabla\phi. \tag{2}$$

For cylinder coordinates, consider a round conductor with a radius a along the z-direction, surrounded by air. Their general solutions for magnetic vector potential in conductor and air are as follows:

$$A_c = A_0 + \sum_{n=0}^{+\infty} J_n(k_2 r)\left(A'_{1n}\cos(n\varphi) + B'_{1n}\sin(n\varphi)\right) \tag{3}$$

$$A_{\text{air}} = C_0 + D_0 \ln(r/r_0)$$
$$+ \sum_{n=1}^{+\infty} \begin{matrix} r^n\left(A'_{2n}\cos(n\varphi) + B'_{2n}\sin(n\varphi)\right) \\ +r^{-n}\left(A''_{2n}\cos(n\varphi) + B''_{2n}\sin(n\varphi)\right) \end{matrix} \tag{4}$$

where A_0 is the particular solution for excitation current, and $k_2 = k_1^* = (1-j)/\delta$, * represents conjugate, $\delta = (2/\omega\sigma_c\mu_c)^{1/2}$ is the skin depth, J_n represents the n order first kind of Bessel function. Based on the boundary conditions, Ampere's law, and the idea of emission and reception [13], multi-conductor matrix equations are built. The coefficient D_0 is equal to $-\mu_0 I/2\pi$, where I is the current the conductor carries. Coefficients C, A'_n, and B'_n are unknown. The detail of the matrix is introduced in Appendix

$$\begin{pmatrix} I_{2N+1} & \cdots & \alpha_{1M} \\ \vdots & \ddots & \vdots \\ \alpha_{1M} & \cdots & I_{2N+1} \end{pmatrix} \begin{pmatrix} \gamma_1 \\ \vdots \\ \gamma_M \end{pmatrix} = \begin{pmatrix} \sum_{j\neq 1}\beta_j + \beta_{\text{ext}} \\ \vdots \\ \sum_{j\neq M}\beta_j + \beta_{\text{ext}} \end{pmatrix}. \tag{5}$$

Matrix α_{ij} represents the contribution from j conductor to i conductor and $i \neq j$. N is truncated order of infinite series in (4). Each submatrix's size is $(2N+1) \times (2N+1)$, and all the diagonal sub-matrixes are identity matrixes. Vector γ_j is a vector composed of unknown coefficients C, A'_n and B'_n. Vector β_j is the contribution from coefficients D_j. Vector β_{ext} is the contribution from the external magnetic field (H_x, H_y).

All coefficients in (3) and (4) can be determined by solving (5). The voltage drop on unit length can be obtained through (6), where S is the cross section area of the conductor. Then, the impedance is obtained

$$-\nabla\phi = R_{\text{dc}}I + \frac{\oiint j\omega A\, dS}{S}. \tag{6}$$

Besides, because external magnetic field performance is more like a controlled voltage source, the impedance of the strands does not include this part of the losses. Therefore, the Poynting vector N based on (7) is used to calculate the losses

$$P = \oint \nabla \cdot N ds = \frac{I^2}{\sigma S} + j\omega\frac{\mu I^2}{2\pi}\frac{J_2(k_2 a)}{ak_2 J_2(k_2 a)}$$
$$+ \frac{j\pi\omega}{\mu}\sum_n \left\{ \begin{matrix} na^{2n}(1 + \frac{J_{n+1}(k_2 a)}{J_{n-1}(k_2 a)})(1 - \frac{J_{n+1}(k_1 a)}{J_{n-1}(k_1 a)}) \\ \times (A'_{2n}A'^*_{2n} + B'_{2n}B'^*_{2n}) \end{matrix} \right\} \tag{7}$$

C. Loss Calculation

In order to calculate the losses in the Litz wire, strand current allocation and external magnetic field are needed. For the external magnetic field, the static magnetic field is considered. In other words, the change of the field due to eddy current is neglected, which is acceptable when Litz wire is chosen properly, i.e., strand radius is small enough compared to skin depth. The field strength can be calculated with FEM or the method of images, and it depends on which method suit the application more. There field results differ from case to case.

Strand current allocation is an important question in the Litz wire. The uneven current distribution can cause much larger eddy current loss than the results from the ideal assumption. The allocation of strand currents is solved by computing the impedance matrix between the strands [10]. The impedance matrix is obtained from the impedance matrix and the length of each cross section area, like (8), where c represents the difference cross section area. The impedance matrix of each cross section is obtained by (6) through setting one strand's current as 1 A and others as 0 A one by one. The induced voltage due to the external magnetic field can also be calculated in the same way. The induced voltage of one cross section area is solved by setting all strand current as 0 A. During calculating the induced voltage, the proximity effect loss in strands is also obtained by (7). Then, the current allocation can be obtained by equating the voltage drop on each strands. Finally, the loss can be calculated by current, impedance matrix and the proximity effect loss in strands. The whole process is shown in Fig. 3

$$Z_{\text{pitch}} = \sum_c Z_{\text{ac}}(c) \times l(c). \tag{8}$$

III. CASE STUDY

There are two cases. One is a two-level twisted wire, which is twisted in both radial and azimuthal directions. It has 3×3 strands, strand radius is 0.1 mm, the insulation layer is 10 μm, and the pitch is 10 mm. Another is a one-level twisted wire, which only be twisted in the radial direction.
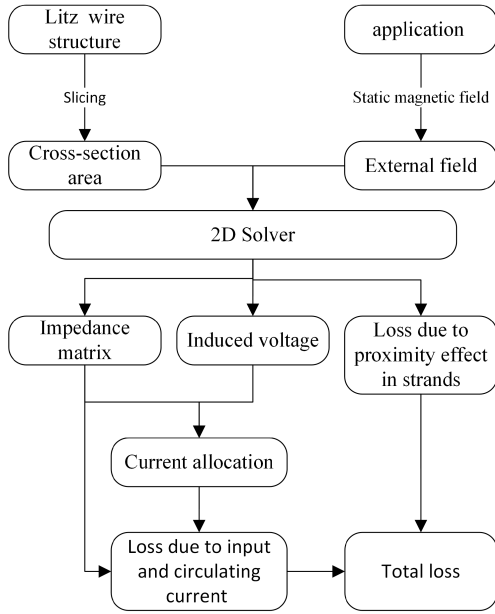
Fig. 3. Flowchart for proposed method.

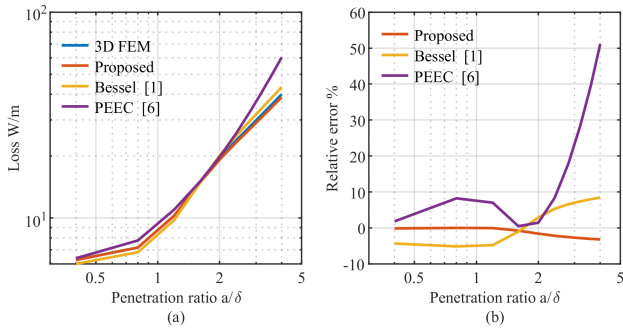Fig. 4. Structure (a) case 1 and (b) case 2.

Fig. 5. Case1: (a) loss per meter and (b) relative error due to excitation current.

It has 11 strands. The radius, insulation thickness, and pitch are the same as in the first case. The structures are shown in Fig. 4.

Results from 3-D FEM are set as a reference, and 3-D FEM is established and solved by COMSOL software. Loss due to excitation current is calculated by assigning 1 A to litz wire. Loss due to external magnetic field is calculated based on 1 A/m external field. Besides the results from 3-D FEM, a classic method [1] and a PEEC method [7] are compared. Detail of 3-D FEMs are shown in Table I, and the proposed method has much faster computational time than 3-D FEM and PEEC.

The results for Case 1 are shown in Figs. 5 and 6. Fig. 5 shows the loss due to excitation current. All three methods have good accuracy compared to 3-D FEM, when penetration ratio $a/\delta < 2$. Case 1 is twisted in both radial and azimuthal directions, which leads to roughly average current distribution in each strand. Therefore, there is no current distribution problem. Fig. 6 shows the loss due to external magnetic field.
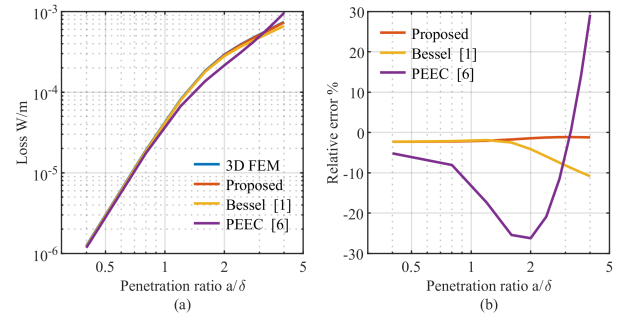

Fig. 6. Case1: (a) loss per meter and (b) relative error due to external magnetic field.

TABLE I
DETAILS OF DIFFERENT METHODS

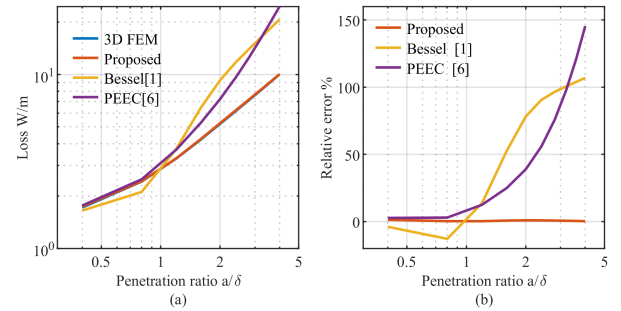| Items	Case 1	Case 2
FEM element number	506267	331818
FEM element average quality	0.6944	0.5148
FEM computational time	2404.6min	2086.4min
Proposed method computational time	0.63s	0.77s
PEEC computational time	227.1s	220.5s

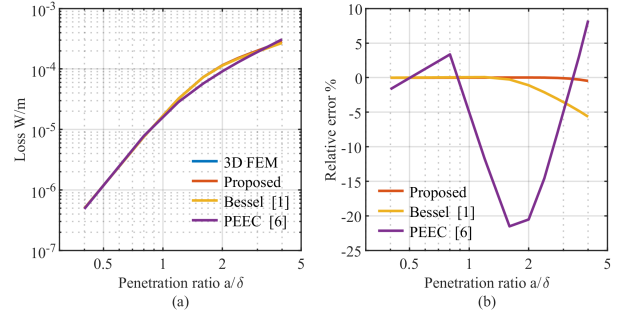Fig. 7. Case2: (a) loss per meter and (b) relative error due to excitation current.

Fig. 8. Case2: (a) loss per meter and (b) relative error due to external magnetic field.

Compared to the proposed and classic methods, the PEEC method underestimate the loss around 14%, when a/δ is 1. It may be because the fineness of filament discretization, which leads to errors in current distribution calculation.

For case 2, the results from different methods are shown in Figs. 7 and 8. In Fig. 7, the loss due to excitation current is calculated with different methods. The classic method shows worse performance in Case 2. Because the wire is only twisted in the azimuthal direction, the strand current in the inner strands and outer strands is not the same, which makes the assumption in the classic method does not valid. Fig. 8 shows the loss due to external magnetic field. Methods considering current distribution show a similar performance as the classic

method, because there is an integer pitch and the induced voltage does not have much difference between strands.

In general, the proposed method provides good accuracy in a wider frequency range. PEEC provides accurate results when penetration ratio $a/\delta < 1$. Besides, the classic method also has good results in Case 1 because it complies with equal current distribution assumption.

IV. Conclusion

This article proposed a loss calculation method for round Litz wires. The method converts 3-D Litz wire into several 2-D cross section. Then 2-D quasi-magnetic field problem is solved in an analytical way based on the magnetic vector potential. The used analytical way does not need discretization procedure and leads to fast computational time. The impedance matrix of litz wire is solved and used to calculate strand current allocation. Two case studies are done, the proposed method has good accuracy and fast computational speed in both cases compared to 3-D FEM. The classic method can be applied to cases like case 1, which twisted in both radial and azimuthal directions.

Appendix
Detail of Matrix

In this appendix, the sub-matrices α_{ij}, β_{ij}, and γ_i used in the model construction are given. In each matrix, symbols n and m change from 1 to N. $\Delta X_{ij} = X_j - X_i$ and $\Delta Y_{ij} = Y_j - Y_i$, which represents the difference in coordinates

α_{ij}

$$
= \begin{pmatrix}
0 & \overbrace{\lambda_{jn}\Re_{ijn0} \quad \cdots}^{N} & \overbrace{\lambda_{jn}\Im_{ij10} \quad \cdots}^{N} \\
0 & \lambda_{jn}P_{nm}\Re_{ijnm} \quad \cdots & \lambda_{jn}P_{nm}\Im_{ijnm} \quad \cdots \\
\vdots & \vdots \quad \ddots & \vdots \quad \ddots \\
0 & -1^{N_r}\lambda_{jn}P_{nm}\Im_{ijnm} \quad \cdots & -1^{N_r}\lambda_{jn}P_{nm}\Re_{ijnm} \quad \cdots \\
\vdots & \vdots \quad \ddots & \vdots \quad \ddots
\end{pmatrix}
$$
(9)

β_{ij}

$$
= \begin{pmatrix}
D_j/2 \ln \dfrac{\Delta X_{ij}^2 + \Delta Y_{ij}^2}{r_0^2} \\
-\dfrac{D_j}{m}\mathrm{Re}((\Delta X_{ij} - j\Delta Y_{ij})^{-m}) \\
\vdots \quad m = 1, 2, \ldots, N \\
-\dfrac{D_j}{m}\mathrm{Im}((\Delta X_{ij} - j\Delta Y_{ij})^{-m}) \\
\vdots \quad m = 1, 2, \ldots, N
\end{pmatrix}
$$
(10)

β_{ext}

$$
= \begin{pmatrix}
-\mu_0(H_x x - H_y y) \\
-\mu_0 H_y \\
0 \\
\vdots \\
\mu_0 H_x \\
0 \\
\vdots
\end{pmatrix}
$$
(11)

γ_i

$$
= \begin{pmatrix}
C_i \\
N\begin{cases} A'_{i1} \\ \vdots \end{cases} \\
N\begin{cases} B'_{i1} \\ \vdots \end{cases}
\end{pmatrix}
$$
(12)

λ_{jn}

$$
= \frac{a_j^{2n} J_{n+1}(k_2 a_j)}{J_{n-1}(k_2 a_j)}, \quad P_{nm} = \frac{(n + m - 1)!}{(n - 1)!m!}
$$

$\Re_{ijnm}$

$$
= \mathrm{Re}\left(\frac{-1^n}{(\Delta X_{ij} - j\Delta Y_{ij})^{n+m}}\right)
$$

$\Im_{ijnm}$

$$
= \mathrm{Im}\left(\frac{-1^n}{(\Delta X_{ij} - j\Delta Y_{ij})^{n+m}}\right).
$$
(13)

Acknowledgment

References

[1] J. A. Ferreira, "Analytical computation of AC resistance of round and rectangular Litz wire windings," *IEE Proc. B Electric Power Appl.*, vol. 139, no. 1, p. 21, 1992.

[2] C. R. Sullivan, "Optimal choice for number of strands in a Litz-wire transformer winding," *IEEE Trans. Power Electron.*, vol. 14, no. 2, pp. 283–291, Mar. 1999.

[3] K. Niyomsatian, J. Gyselinck, and R. V. Sabariego, "Closed-form complex permeability expression for proximity-effect homogenisation of Litz-wire windings," *IET Sci., Meas. Technol.*, vol. 14, no. 3, pp. 287–291, May 2020.

[4] T. Ewald and J. Biela, "Analytical winding loss and inductance models for gapped inductors with Litz or solid wires," *IEEE Trans. Power Electron.*, vol. 37, no. 12, pp. 15127–15139, Dec. 2022.

[5] C. R. Sullivan and R. Y. Zhang, "Analytical model for effects of twisting on Litz-wire losses," in *Proc. IEEE 15th Workshop Control Model. Power Electron. (COMPEL)*, Jun. 2014, pp. 1–10.

[6] E. Plumed, J. Acero, I. Lope, and C. Carretero, "3D finite element simulation of Litz wires with multilevel bundle structure," in *Proc. 44th Annu. Conf. IEEE Ind. Electron. Soc. (IECON)*, Oct. 2018, pp. 3479–3484.

[7] R. Y. Zhang, J. K. White, J. G. Kassakian, and C. R. Sullivan, "Realistic Litz wire characterization using fast numerical simulations," in *Proc. IEEE Appl. Power Electron. Conf. Expo. (APEC)*, Mar. 2014, pp. 738–745.

[8] J. Lyu, H. C. Chen, Y. Zhang, Y. Du, and Q. S. Cheng, "Litz wire and uninsulated twisted wire assessment using a multilevel PEEC method," *IEEE Trans. Power Electron.*, vol. 37, no. 2, pp. 2372–2381, Feb. 2022.

[9] S. Ehrlich, H. Rossmanith, M. Sauer, C. Joffe, and M. März, "Fast numerical power loss calculation for high-frequency Litz wires," *IEEE Trans. Power Electron.*, vol. 36, no. 2, pp. 2018–2032, Feb. 2021.

[10] T. Guillod, J. Huber, F. Krismer, and J. W. Kolar, "Litz wire losses: Effects of twisting imperfections," in *Proc. IEEE 18th Workshop Control Model. Power Electron. (COMPEL)*, Jul. 2017, pp. 1–8.

[11] G. Cerri, V. M. Primiani, and S. A. Kovyryalov, "Modelling of a Litz-wire planar winding geometry for an accurate reactance evaluation," *IET Sci., Meas. Technol.*, vol. 4, no. 4, pp. 214–219, Jul. 2010.

[12] E. Plumed, I. Lope, C. Carretero, and J. Acero, "A recursive methodology for modelling multi-stranded wires with multilevel helix structure," *Appl. Math. Model.*, vol. 83, pp. 76–89, Jul. 2020.

[13] T. Delaforge and H. Chazal, "Formal solution based on the magnetic potential for round conductive area," *IEEE Trans. Magn.*, vol. 54, no. 12, pp. 1–8, Dec. 2018.